SLAC – PUB – 4484
November 1987
(M)

POSITRONS FOR LINEAR COLLIDERS*

STAN ECKLUND
Stanford Linear Accelerator Center
Stanford, California 94305

TABLE OF CONTENTS

1. REQUIREMENTS 2
2. METHODS OF POSITRON PRODUCTION 2
3. ELECTROMAGNETIC CASCADE SHOWERS 3
4. CROSS SECTION FOR PAIR, COMPTON 3
5. THE EGS PROGRAM 4
6. GENERAL OVERVIEW OF POSITRON DISTRIBUTIONS . 4
7. PHOTONS FROM SYNCHROTRON RADIATION 8
8. PHOTONS FROM CHANNELING 8
9. POSITRON COLLECTION 11
10. TRANSVERSE FOCUSING TECHNIQUES 12
11. LONGITUDINAL CAPTURE 13
12. COMPUTER RAY TRACING 14
13. SPACE-CHARGE EFFECTS 15
14. THERMAL HEATING AND STRESS DUE TO SHOWER . 15
REFERENCES 23

*Work supported by the Department of Energy, contract DE–AC03–76SF00515.

Invited talk presented at the U.S. Summer School on High Energy Particle Accelerators, Batavia, Illinois, August 13–24, 1984

1. REQUIREMENTS

In general, the requirements of a positron source for a linear collider are similar to those for the electron source. This arises because of intensity limits caused by wake fields in the linac structure and the desire to maximize the luminosity of the machine. For example, if the luminosity limiting factor is wake field disruption of the beams, one would push to that limit with both positrons and electrons. In the usual case where the method of production uses an electron beam to initiate the positron production process, a system with a yield or efficiency greater than or equal to one is needed.

Ultimately, a low emittance beam is needed for small size beams at the interaction region. Most positron sources give adequate numbers of particles into extremely large emittances; hence the need for emittance reduction in one or several damping rings. However, the positron beam emittance must be suitable for injection into a reasonable damping ring. We must consider the full six–dimensional phase volume (coordinates: x, x', y, y', dP/P, dz). Both the transverse (x, x') or (y, y') and the longitudinal $(dP/P,\ dz)$ emittances present challenges to the design and realization of an adequate positron system.

Another important factor in obtaining large luminosity for a linear collider is to produce a high instantaneous current (small dz spread). This requires a positron source with the particular time structure desired or a storage device to collect and periodically release the charge.

2. METHODS OF POSITRON PRODUCTION

Positrons are not stable in matter because of their annihilation with atomic electrons. As a source for accelerators, positrons are normally produced by electromagnetic interactions, namely by pair production from a photon in the field of the nucleus. Positrons also are readily available by nuclear beta decay via the weak interactions. Relatively hot sources would be required to achieve intensities required for linear colliders. Also, because of its random time structure, beta decay is most useful as a source of positrons when a continuous beam is desired. The pair production process has the advantage of being essentially instantaneous, allowing production of beams with a time structure or bunching required for the linear collider. For sources which use pair production, the varieties of design depend on the method of obtaining photons.

3. ELECTROMAGNETIC CASCADE SHOWERS

The most common method to produce the required photons is by an electromagnetic cascade shower. Usually an electron beam is used to initiate the shower. The multiplication process involving Compton scattering, bremsstrahlung, and pair production is well-known[1] and is calculated in excellent detail for particular geometries by a Monte Carlo computer program.[2] The particle multiplication ratio can be in the hundreds for incident beams of tens of GeV, which provides an easy way to obtain large numbers of positrons, albeit in rather large phase-space volumes.

4. CROSS SECTION FOR PAIR, COMPTON

Cross sections for the electromagnetic cascade shower processes of positron-electron pair production and Compton scattering are shown in Fig. 1.

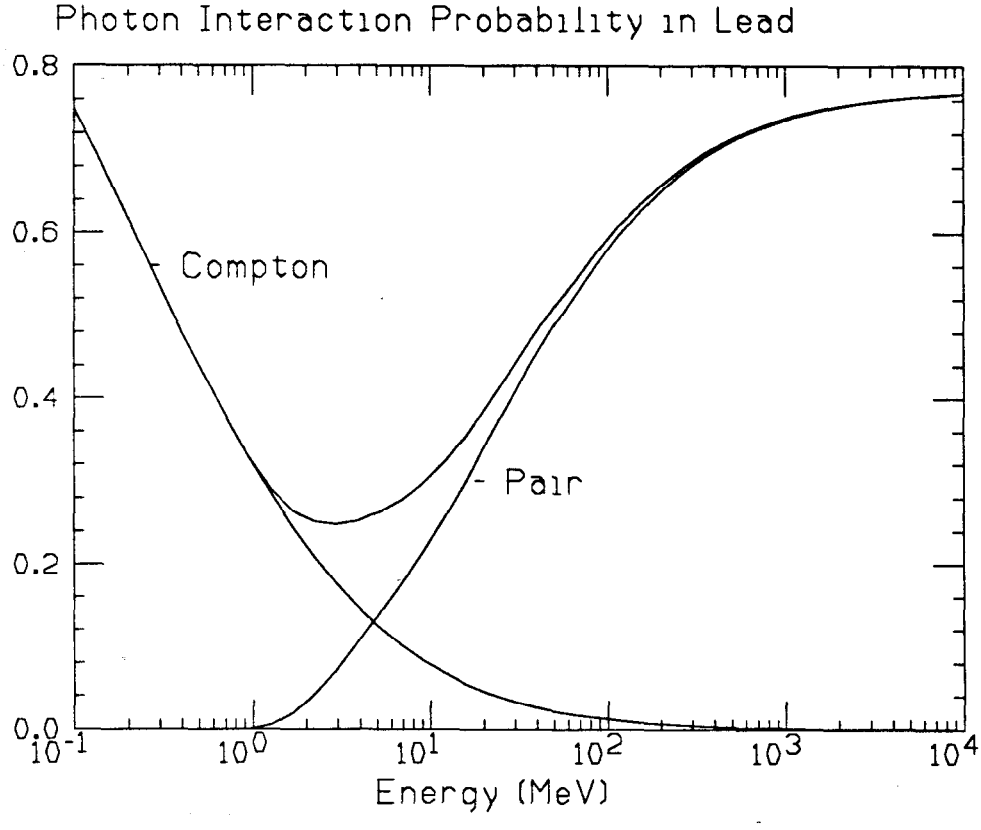

Fig. 1. Probability per radiation length of e^+e^- pair production and Compton scattering as a function of photon energy. These data come from the EGS program.

Note that pair production, which is the supplier of positrons, is of a good magnitude above 50 to 100 MeV. This means that, practically, incident beam energies should be at least that high or the efficiency of the system will be low.

5. THE EGS PROGRAM

The electromagnetic cascade is sufficiently complicated so that a computer Monte Carlo program is the efficient way to obtain meaningful results for a particular geometry. A program called EGS is commonly used for this purpose. Actually two separate programs are used; PEGS, which calculates cross sections and makes appropriate tables, and the main EGS code, which does the Monte Carlo particle tracking for the geometry of interest. PEGS is specific to a particular element, compound, or mixture of compounds and an energy range. Pegs is usually run only once at the beginning of solving a problem (or not at all if one of the standard files can be used), and EGS numerous times for the various geometries, energies, *etc.*, of interest. The majority of the EGS program is "standard code," but the user must write a portion of the code which is descriptive of the geometry of the problem to be solved, the incident beam conditions, and the output desired from the program. For many cases and those reported here, a simple cylindrically symmetrical geometry with infinite slabs, of thickness one radiation length, perpendicular to the beam axis will be used. Positron yields will be a function of positron momentum or energy (three components), and position, as well as the initial conditions.

6. GENERAL OVERVIEW OF POSITRON DISTRIBUTIONS

Outputs from a variety of EGS computer runs are given here to provide a characterization of the positron beam emerging from a thick production target. In the following, E is the energy of the positron in MeV, x, y, z are the position of the positron in cm, where the incident beam is parallel to the z axis, and P_x, P_y, P_z are components of the momentum of the positron in units of MeV/c. Figures 2 to 7 are calculated from EGS output for an incident electron beam of energy 33 GeV, incident upon a tungsten target.

Several properties of the positron distributions are worth noting since they relate to the number and phase-space volume of positrons. First note that yields substantially greater than unity are realizable for an energy as large as 33 GeV. The energy spread, however, is large and characteristic of a $1/E$ distribution. The transverse size of the positrons in a dense target is small, of order 1 mm, which is good from a phase-space point of view but bad for target stress and pulse heating. The transverse momentum appears dominated by multiple scattering, almost independent of z, but dependent on the high energy cut of the sample considered. Correlations in transverse phase-space (*i.e.*, x, P_x) are present at about the 20% level, which may be significant but not terribly useful. Note that this correlation simply reflects that the effective source z location is a finite distance up-beam of the target down-beam face where the positron trajectories are tabulated.

The yield dependence on atomic number is especially striking and is due to a lower critical energy for high–Z materials. Effectively the positron or electron energy loss per radiation length

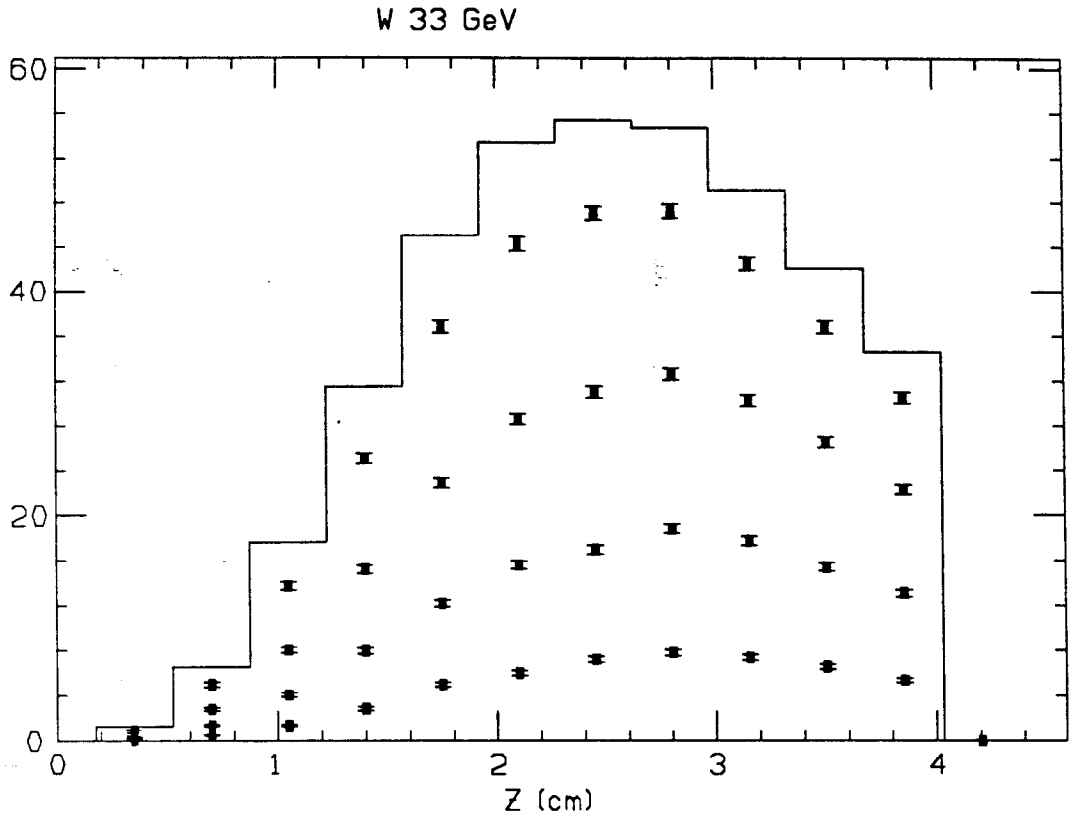

Fig. 2. Positron flux in tungsten per incident electron vs z for incident energy of 33 GeV. The different curves are for successively bigger cutoffs in maximum positron energy of 5, 10, 20, 50, and 100 MeV. The minimum energy cutoff is 2 MeV. The z bins are one radiation length. Note the shower maximum is around seven radiation lengths for this energy. The calculation covers the first eleven radiation lengths.

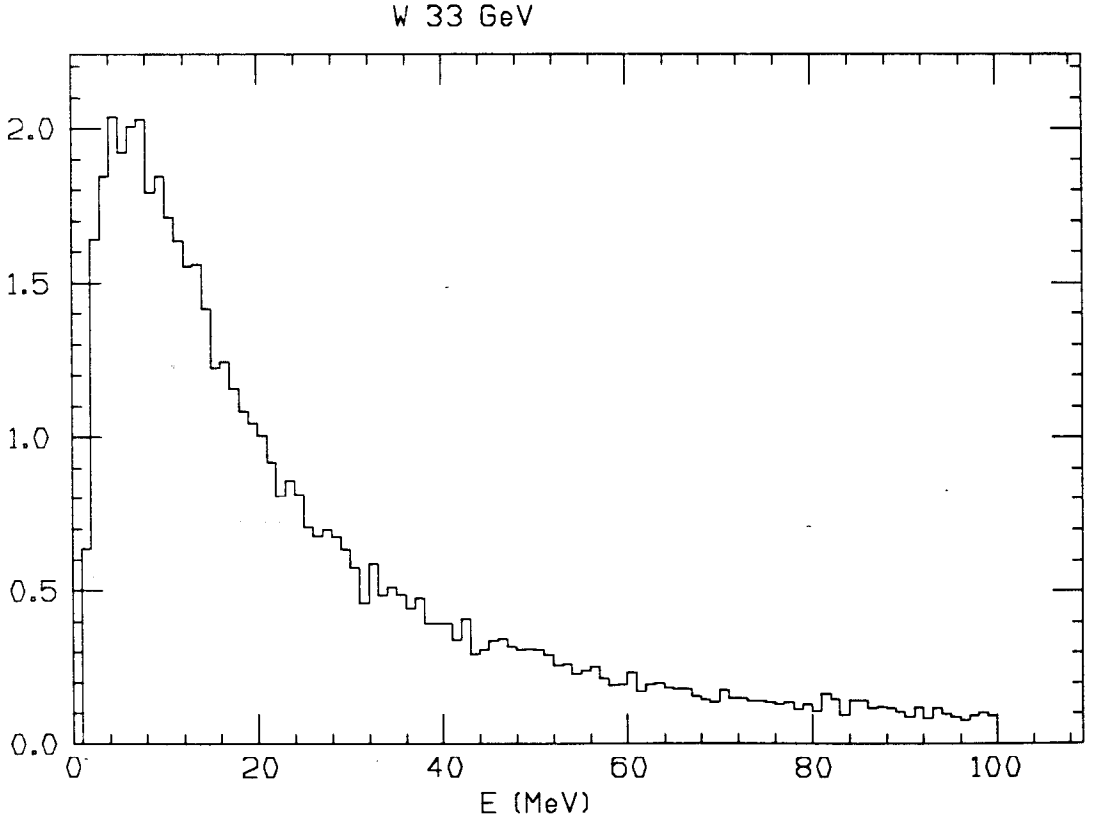

Fig. 3. Yield per 1–MeV energy (E) bin versus E at $z = 6$ radiation lengths.

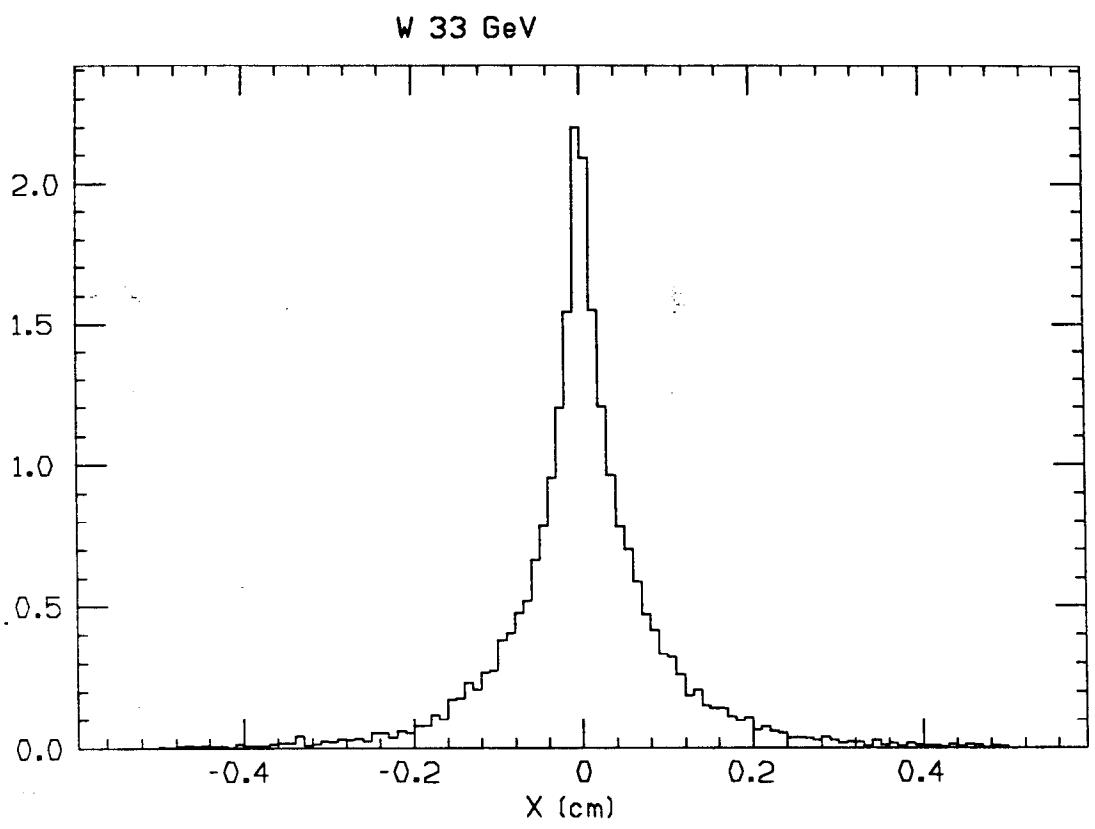

Fig. 4. Yield per 0.01–cm bin versus x at $z = 6$ radiation lengths.

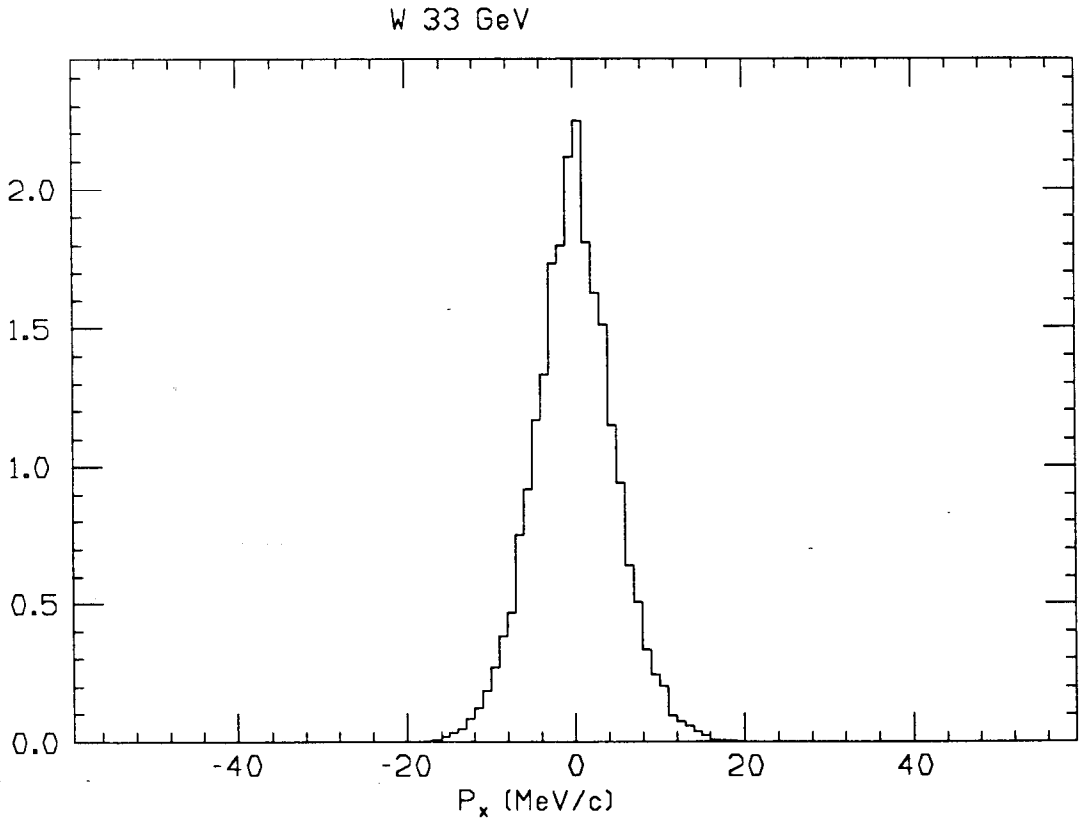

Fig. 5. Yield per 1–MeV bin versus P_x at $z = 6$ radiation lengths.

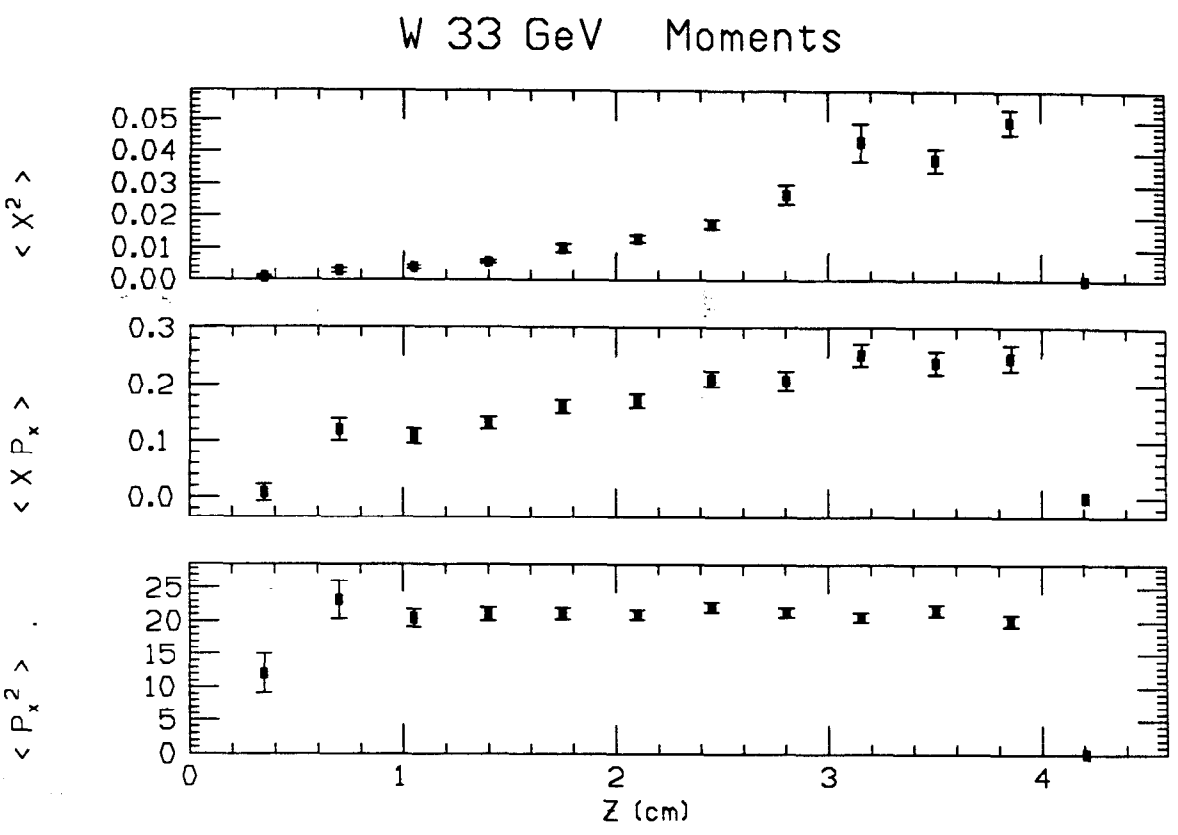

Fig. 6. Moments in x, P_x versus z for $5 \leq E \leq 20$ MeV.

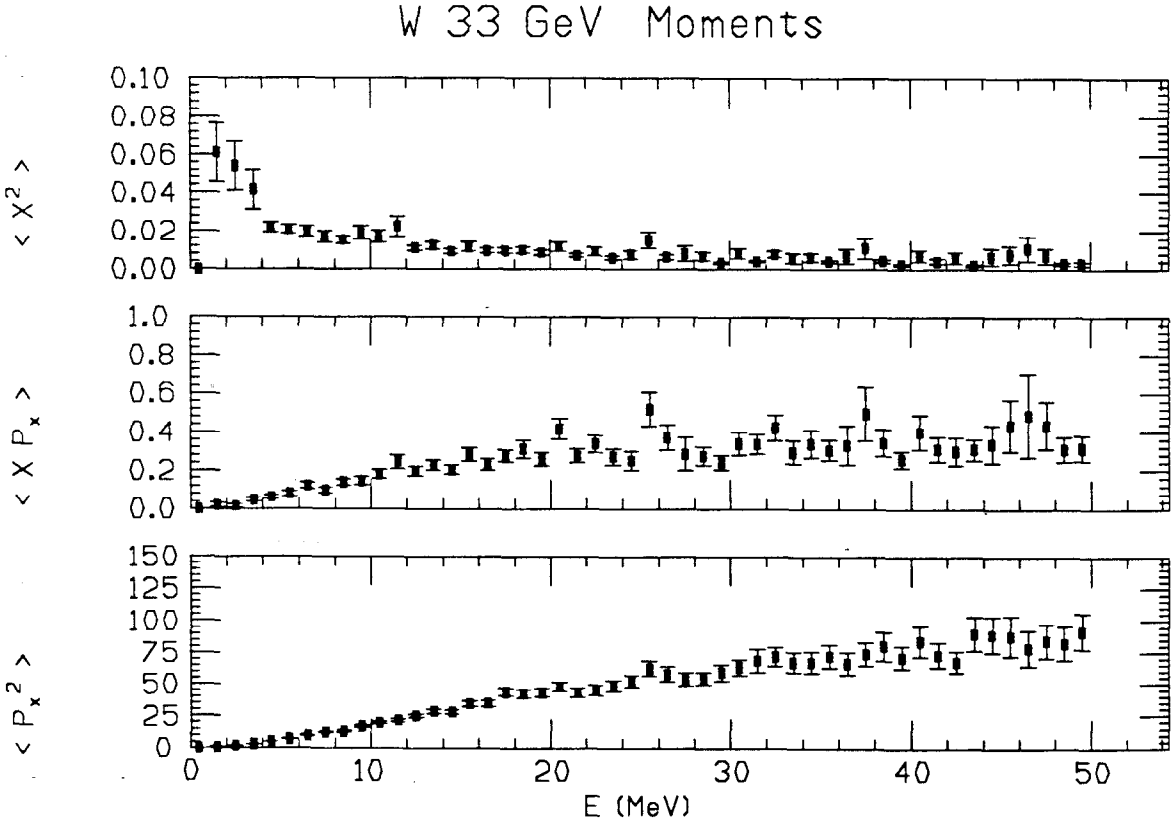

Fig. 7. Moments in x, P_x versus E for $z = 6$ radiation lengths.

is less in high–Z materials. Table I shows the data from an EGS run which illustrates this effect for copper and tungsten at 17– and 50–GeV incident beam energies. Also note that the higher–Z material results in a desirable smaller phase-space of positrons due to a smaller beam size.

Table I. Positron Yield Properties from Copper and Tungsten

Incident Energy:	17 GeV		50 GeV	
Material	Cu	W	Cu	W
Radiation Length	14.3	3.5	14.3	3.5
Yield at $z = 6$ r.l. for $2 < E < 5$	2.8	5.8	7.4	13.4
σ_x (mm)	2.1	1.1	1.8	1.1
σ_{P_x} (MeV/c)	3.0	3.3	3.0	3.5

Of interest and possibly relevant for high energy linear colliders are the yields with higher energy electron beams. The relevancy will of course depend on the practicality of using a spent beam after collision or accelerating extra scavenger electron bunches to initiate an electromagnetic cascade shower in a thick target. Figures 8 to 12 summarize an EGS calculation with 1–TeV electrons incident on a thick tungsten target. Results are shown at six-radiation-lengths depth into the shower and at shower maximum, which occurs at ten radiation lengths. The yields obtainable are large because of the high multiplication of the shower. Note, however, that the properties of the positrons are quite similar to the properties at 33 GeV.

7. PHOTONS FROM SYNCHROTRON RADIATION

In the case of a high energy collider, an attractive method to obtain photons is to pass the spent electron or positron beam (after collision) through an alternating magnetic field called a wiggler or undulator.[3] The photons produced by synchrotron radiation are then impinged on a thin target where pair production provides the positrons. It is required, of course, to produce a large quantity of photons of sufficient energy to be above threshold for this production process. An important benefit from this method is that, by using a helical undulator, circular polarized photons are obtained and from them polarized positrons. To obtain an adequate number of positrons (yield ratio of unity or better) via synchrotron radiation, a beam energy of at least 100 GeV and a long (300–meter) wiggler magnet with high field (1 Tesla) is needed.[4] Probably this method will be useful for colliders with beam energies above 200 GeV.

8. PHOTONS FROM CHANNELING

Another method to obtain an enhanced photon flux is via channeling of electrons in a crystal. Enhancements of order 10 to 100 over ordinary bremsstrahlung have been calculated.[5]

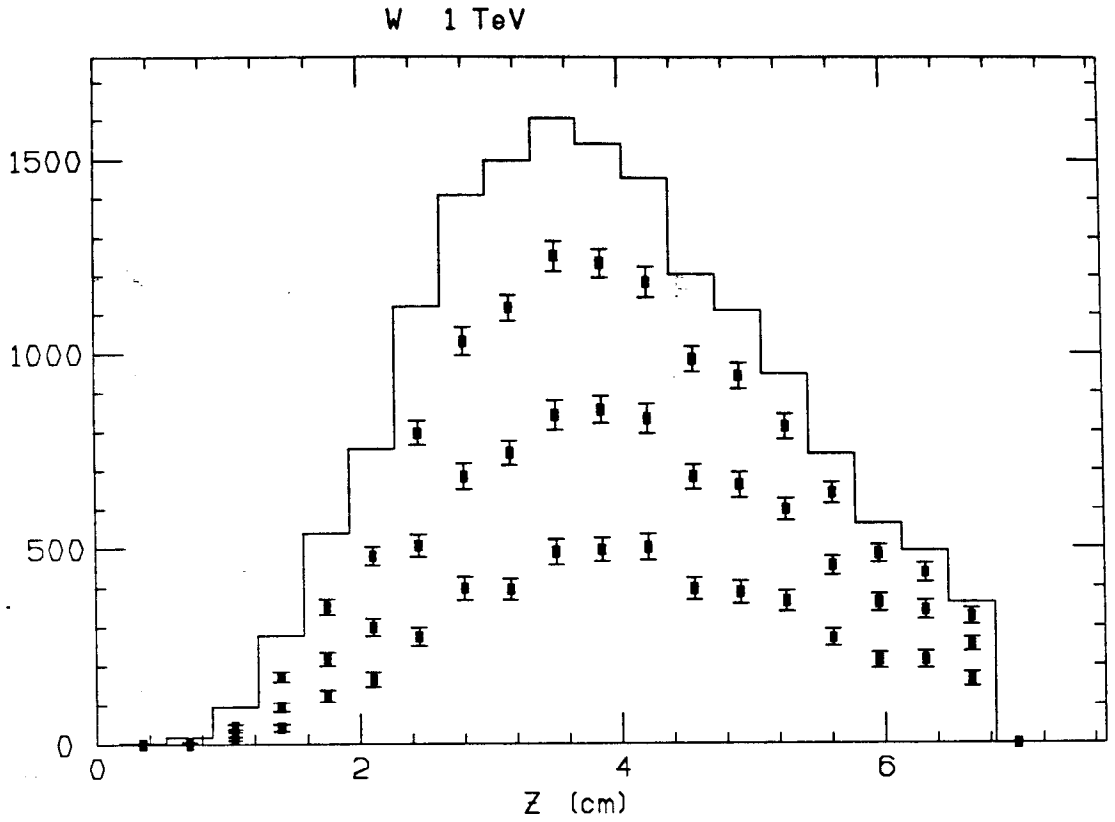

Fig. 8. Total positron yield versus z for positron energies, $E < 10$, 20, 50, and 1000 MeV.

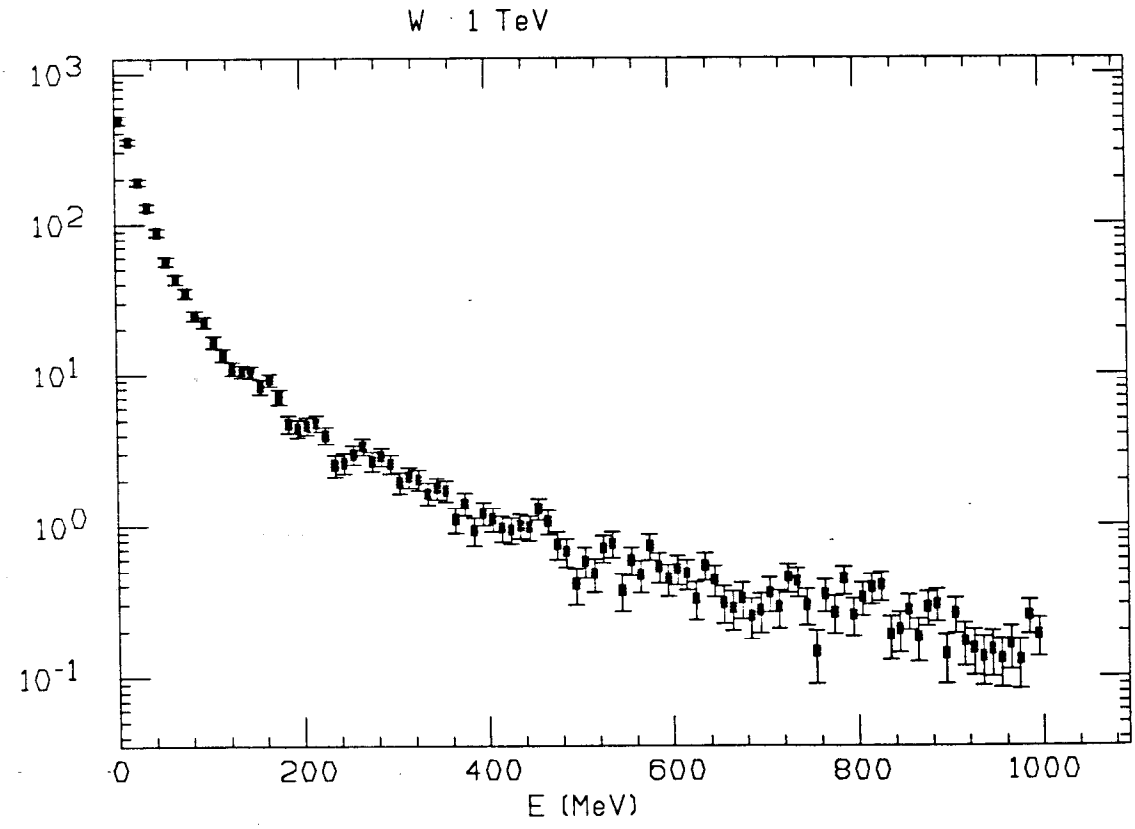

Fig. 9. Positron yield per 10–MeV bin versus E at $z = 10$ radiation lengths.

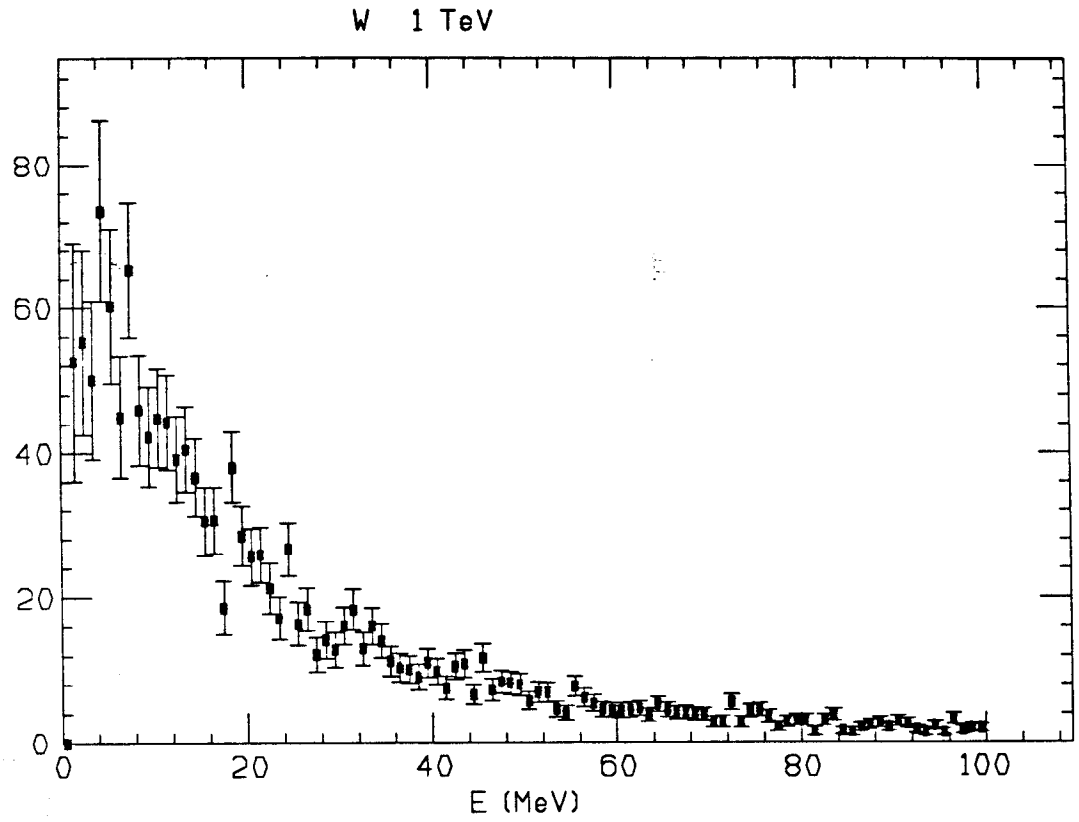

Fig. 10. Positron yield per 1–MeV bin versus E at $z = 10$ radiation lengths.

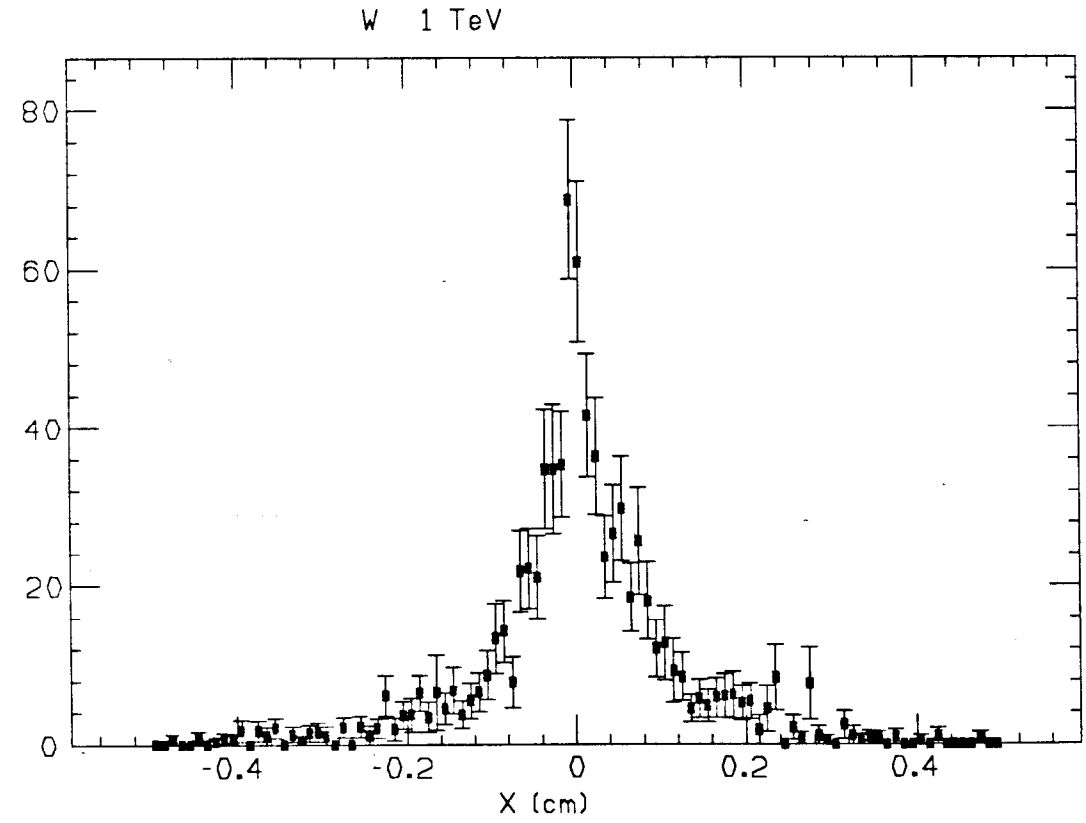

Fig. 11. Yield per 0.01–cm bin versus x at $z = 10$ radiation lengths.

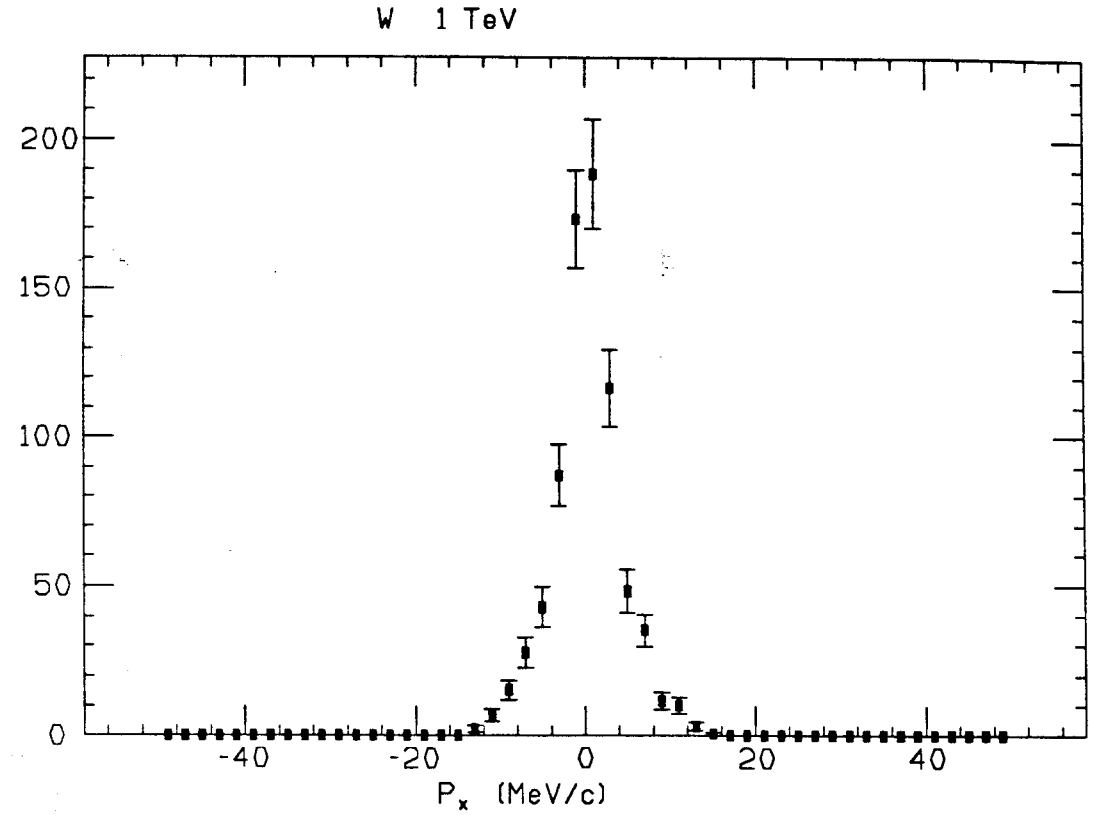

Fig. 12. Positron yield per 2–MeV/c bin versus P_x at $z = 10$ radiation lengths.

This method can be thought of as using an atomic wiggler, which provides strong electric fields in crystal planes. Channeling may prove to be useful for positron production, but a number of practical problems would need to be solved such as radiation damage to the crystal.

9. POSITRON COLLECTION

A major task in a positron source design is efficient collection of the positrons coming out of the target. The phase-space distributions shown in the figures reveal large energy ranges like 2 to 20 MeV and large angular divergences. The large energy spread leads to the need for wide-band transverse focusing. That is, the focusing must work for a large range of positron energies. Solenoidal fields, which deflect particles in proportion to their transverse momentum, are appropriate when adiabatic or slowly varying. The EGS calculations give beam sizes of order 1–mm radius and transverse momentum up to the energy of the positron, which implies angles of order one radian. If one wanted optical matching of the positron beam coming from a target, it would imply a beta-function of order one millimeter. To achieve such a beta-function value would require extremely strong magnets.

Positrons ultimately must be accelerated and stored in a damping ring in order to reduce their large emittance. The storage or damping ring must operate at an energy that provides

adequate damping, typically about 1 GeV. The acceleration mechanism must efficiently capture the bunch from the target. Given the low energy, not all the positrons are relativistic. It takes some finite acceleration to obtain a fully relativistic beam, during which time the lower energy positrons are falling behind the higher. This leads to an increase in the longitudinal (z) size of the beam and hence the longitudinal emittance. Subsequent acceleration even after the beam is relativistic will usually lead to additional energy spread due to the sine wave shape of the RF accelerating field. This effect, along with the damping ring energy acceptance, then limits the useful number of positrons. Acceleration with high gradient immediately after the target is desirable in most instances. The positron longitudinal capture and damping ring should be designed and optimized as a whole system. Often the longitudinal phase-space can be rotated and matched by use of RF compressors and nonisochronous beam transports to obtain the best overall performance.

10. TRANSVERSE FOCUSING TECHNIQUES

Several types of focusing devices have been proposed and used for collecting positrons. Some provide solenoidal magnetic fields (in the z direction along the beam direction) and others use transverse fields. The simplest configuration is an adiabatically changing solenoidal field. It can be shown[6] that this transforms the phase-space radii by the square root of the magnetic field ratio, *i.e.*, Ba^2 is a constant proportional to beam emittance, where B is the magnetic field and a the beam radius. The final field value, away from the target, must be large enough to keep the beam inside the accelerator aperture. The initial value then needs to be high to achieve a useful transformation of the phase-space aspect ratio. The adiabatic solenoid is probably the best solution except for the limit of the maximum field obtainable, which is usually in the 1– to 2–Tesla range.

Another approach is to use a 1/4–wave transformer. One uses a solenoidal field of strength and length just right to rotate phase space 90° or 1/4 of a cyclotron wave length. This has the advantage of transforming phase-space by the ratio of initial to final magnetic fields, which is a better ratio than for the adiabatic case. The disadvantage is that 1/4–wave is correct only for a unique energy, and a relatively narrow energy band or set of bands is collected. Devices that are compromises between 1/4–wave and adiabatic may offer some kind of an optimum.

A device commonly used to provide a high magnet field is a pulsed flux concentrator.[7] This type of magnet is basically an eddy current transformer that steps up current. Its name comes from the concentration of magnetic flux lines from a large area of a primary coil to a smaller area single-turn secondary. It is made without the aid of magnetic materials and relies on the inability of AC fields to penetrate beyond a skin depth into a metal. As such its efficiency is

strongly dependent upon primary to secondary coupling or conductor spacing. The single-turn secondary is typically a cylinder of copper with a radial slot cut to a central conical hole where the field is concentrated. Neglecting leakage flux, it follows that the field varies inversely with the cross-sectional area of the open conical hole. The small end of the cone is located near the target where the strongest field is desired.

A flux concentrator has been used at SLAC in the SLC positron source to provide 4–Tesla peak fields. Thin 0.2–mm sheets of mica are used for insulation. In time we found in some units an abrasion of the mica, presumably due to mechanical motion of the coil. This leads to voltage breakdown at the higher operating points. Because of this, a new single coil was designed which does not need an insulating material but instead relies on vacuum insulation. It is basically a simple coil with the inside dimensions conical as in the mica insulated design. This results in the same boundary conditions, and therefore the same magnetic field, except for any leakage flux between the turns. The coil is manufactured by wire electronic discharge machining, which results in about 0.25–mm spaces between conductors turns. Even with such small spaces for leakage flux, this device is about 50% less efficient than the design utilizing mica insulation. Its chief advantage is expected to be its durability.

Several types of focusing devices provide azimuthal fields by running a pulsed current in the beam direction. In particular use, both for positron collection and antiproton collection, are lithium lenses. Lithium is chosen as the current-carrying conductor to minimize multiple scattering of the beam. If the current is uniform in the conductor, the magnetic field will increase linearly with radius, providing a linear focusing element. The current is pulsed to reduce the average power, but the pulse length is chosen to obtain good current penetration and a nearly uniform distribution. Currents of order 100 kA are used to achieve fields of 10 Tesla in lenses 1 or 2 cm long. Another variation on focusing with an azimuthal field is the parabolic lens. A current in a wire will produce a field that falls off inversely with radius or distance from the wire. To produce a linear focusing force a parabolic horn-shaped conductor is used which provides a path in the field which increases as the square of the radius.

11. LONGITUDINAL CAPTURE

The longitudinal motion of positrons in the accelerator is relatively straightforward to calculate in the case of negligible motion transverse to the accelerator axis. A constant of the motion can be obtained relating energy and phase of the particle relative to the RF accelerating field.

Let

$$G = \text{accelerator gradient of RF},$$

$$\lambda = \text{RF wavelength},$$

$$\beta_p = \text{phase velocity of RF},$$

$$\phi = \text{phase of particle relative to RF},$$

$$E = \text{energy of particle} \quad ;$$

then

$$d\phi = \frac{2\pi}{\lambda}\left(\frac{1}{\beta_p} - \frac{1}{\beta}\right) dz \,,$$

$$\frac{dE}{dz} = -G \sin\phi \,,$$

give the equations of motion. Combining the two above equations to eliminate z and integrating gives

$$\frac{2\pi}{\lambda}\left(\frac{E}{\beta_p} - \sqrt{E^2 - m^2}\right) = G\,(\cos\phi - \cos\phi_\infty)$$

where $\cos\phi_\infty$ is a constant of integration chosen to correspond to the phase at infinite energy or time. This relation gives the directed path of particle motion in $E\phi$ space under the accelerating field. The parameter for this family of paths is the constant of integration $\cos\phi_\infty$. From an initial bunch of positrons the final asymptotic phase distribution is easily calculated by solving for ϕ_∞. This formulation is convenient, but the approximation of small transverse motion is usually not valid and the full space and time equations must be solved. This usually requires computer ray tracing.

12. COMPUTER RAY TRACING

Depending on the devices used in collection of positrons, the calculation of net yield can be of varying degrees of difficulty. It is convenient to have analytic calculations which lend themselves to an understanding of the quantitative performance of the system. Often, however, in pushing for highest positron yield, one is driven to nonideal devices which may be nonlinear and not adiabatic. Also the positron shower properties need four variables (r, P_r, P_θ, and P_z) to be properly described. The net effect is to make analytic calculations difficult except in idealized cases. Computer ray tracing provides a way to calculate and optimize the performance of the collection system. At SLAC a program named ETRANS[8] has been used to integrate the positrons' trajectories in three-dimensional space and time through a flux concentrator field, slowly varying solenoidal fields, and the acceleration to 200 MeV. The space dependence of fields is taken to be

cylindrically symmetrical. Input trajectories are taken from EGS Monte Carlo positron output trajectories. The output from the program is in the form of histograms of accepted and rejected positrons as a function of input or output space and momentum coordinates. Output trajectories were also used as input to other ray tracing programs such as TURTLE.[9] Space-charge effects were ignored in this program. Computer runs could be made for a variety of collection parameters in order to optimize the positron yield.

13. SPACE–CHARGE EFFECTS

The effects of space charge or wake fields are more difficult to calculate. A program called MASK[10] has been used at SLAC and at several other laboratories to solve for the induced electromagnetic fields and particle transport. Calculating the beam trajectory for as short a time as 40 picoseconds is a significant job for existing computers. In a limited number of runs of the SLC geometry, noticeable space-charge effects were observable only 12 mm from the target for intensities 6×10^{12} positrons. Note that both positrons and electrons are present in nearly equal numbers and must be included in any space-charge calculation. It is fortuitous that the two charges will induce opposite fields which will cancel. Once the positrons and electrons enter the accelerator, however, the positrons and electrons separate and large wake fields will be present.

14. THERMAL HEATING AND STRESS DUE TO SHOWER

A major concern in using a target for production of positrons is whether the target material can withstand the thermal shock caused by the incident beam. Energy loss by ionization locally heats the target, causing an area of stress that propagates as a shock wave in the material. The EGS program can sum the energy deposition in various regions of the target. A convenient quantity is the fractional energy density

$$\frac{1}{E}\,\frac{dE}{dV} \quad ,$$

where E is the total incident beam energy and dE is the energy accumulated in a volume dV. Note that this quantity is independent of the incident beam intensity or power.

The temperature rise in a localized region is given by

$$\Delta T_p = \frac{N\,E_0}{\rho\,C_p}\left(\frac{1}{E}\,\frac{dE}{dV}\right) \quad ,$$

where

N = number of particles in beam pulse ,

E_0 = beam energy ,

C_p = material heat capacity ,

ρ = density .

Examples of EGS runs for 50–GeV electrons incident on Al, Cu, and W target materials are given in Figures 13–24.[11] Note the logarithmic scaling of the radial bins (cylindrical symmetry is assumed about the beam axis). The temperature rises are calculated for $N = 5 \times 10^{10}$ incident electrons. Incident beam sizes of 0.05, 0.10, 0.5, and 1.0 mm are shown by the respective symbols $\times$, $\diamond$, $+$, and $\square$. Note that temperature rises from a single beam pulse can be dangerously large in the case of small beams hitting high–Z materials. A common technique used to reduce the maximum temperature is to use a low–Z material as a spoiler up-beam of the main target material. This spoiler then increases the beam size at the target by multiple scattering but because of its lower density does not itself have too high an energy deposition density.

Although it is easy to find target materials that can stand high temperatures, the problem of excessive stress to the target is often difficult to solve. Solving the stress equation in three dimensions with time dependence of the shock wave after a short beam pulse is seemingly beyond our present computational capabilities. Often the problem is simplified by calculating the maximum stress occurring just after the beam hits the target and assuming the z (beam direction) dependence to be slowly varying. One then can use the stress equations for a long cylinder with axis parallel to the beam direction. For a long cylinder of radius b, the stress equations are[12]

$$\sigma_r = \frac{\alpha E}{1-\nu}\left(\frac{1}{b^2}\int_0^b T(r)\,r\,dr - \frac{1}{r^2}\int_0^r T(r)\,r\,dr\right) ,$$

$$\sigma_\theta = \frac{\alpha E}{1-\nu}\left(\frac{1}{b^2}\int_0^b T(r)\,r\,dr + \frac{1}{r^2}\int_0^r T(r)\,r\,dr - T(r)\right) ,$$

$$\sigma_z = \frac{\alpha E}{1-\nu}\left(\frac{2\nu}{b^2}\int_0^b T(r)\,r\,dr - T(r)\right) ,$$

α = coefficient of expansion ,

E = modules of elasticity ,

ν = Poisson's ratio (typically 0.25–0.3) .

Note that the maximum stress is of order

$$\sigma_{max} = \frac{\alpha\, E\, T_{max}}{2\,(1-\nu)} .$$

This quantity in comparison to the ultimate tensile strength is a figure of merit for selection of materials and judgment of the survivability of a target.

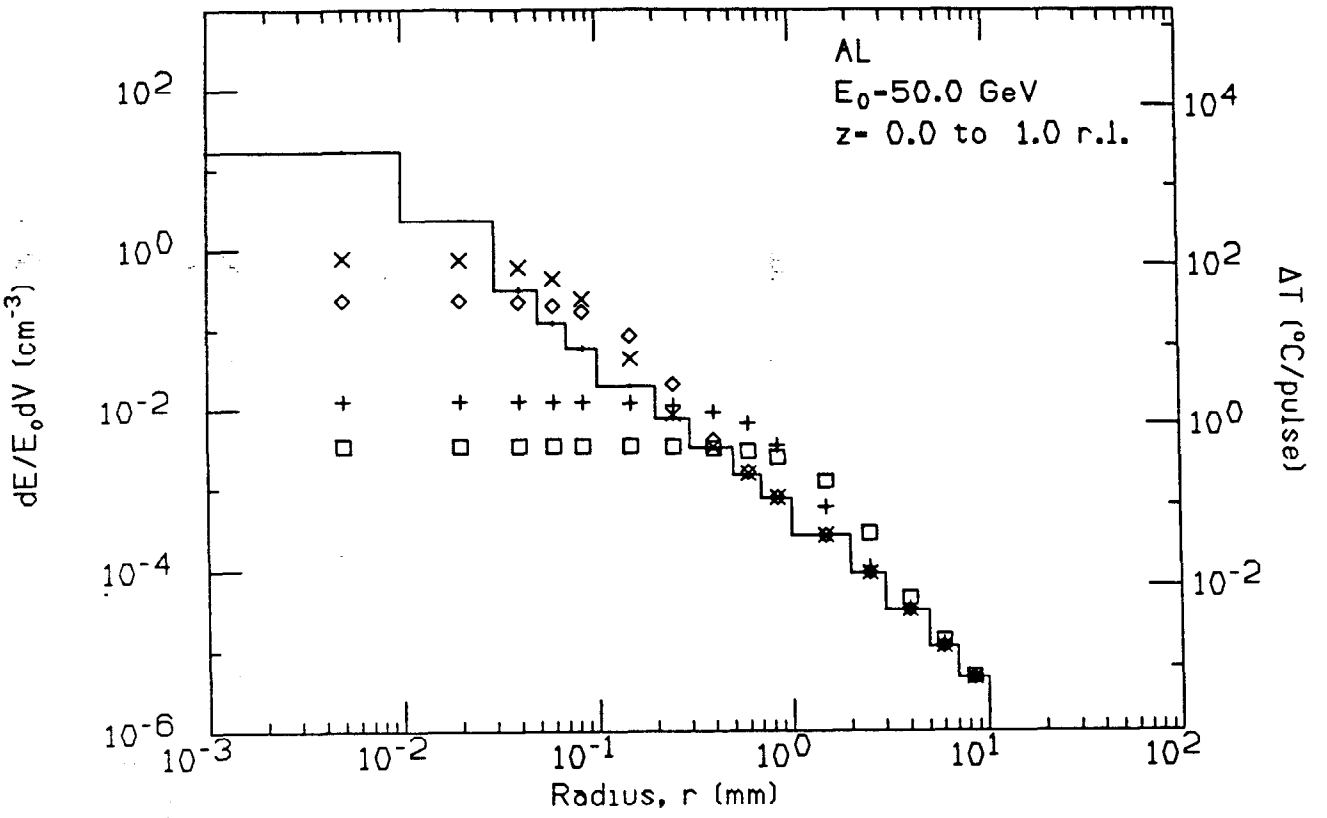

Fig. 13. E–deposition and temperature rise for electron beams of various sizes for aluminum at $0 < z < 1$ radiation lengths.

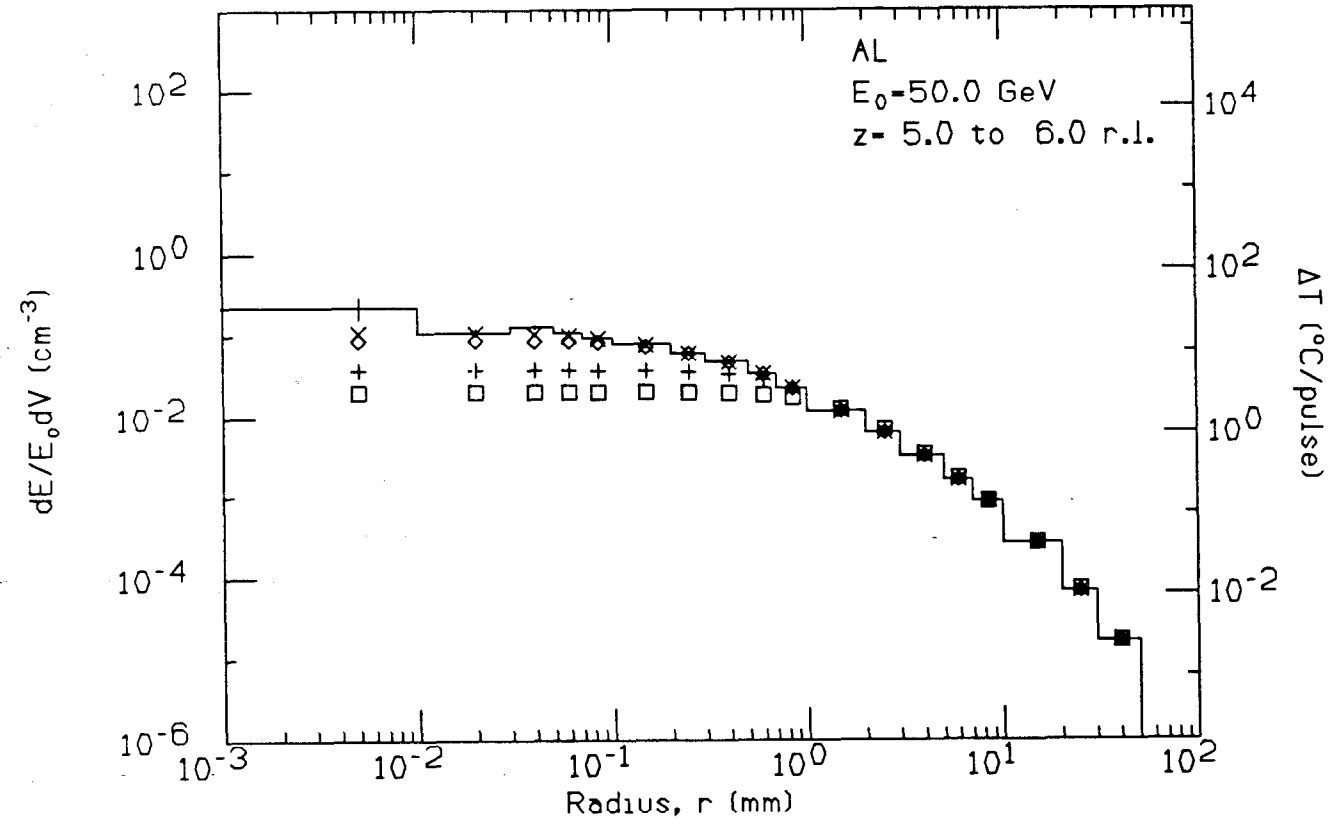

Fig. 14. E–deposition and temperature rise for electron beams of various sizes for aluminum at $5 < z < 6$ radiation lengths.

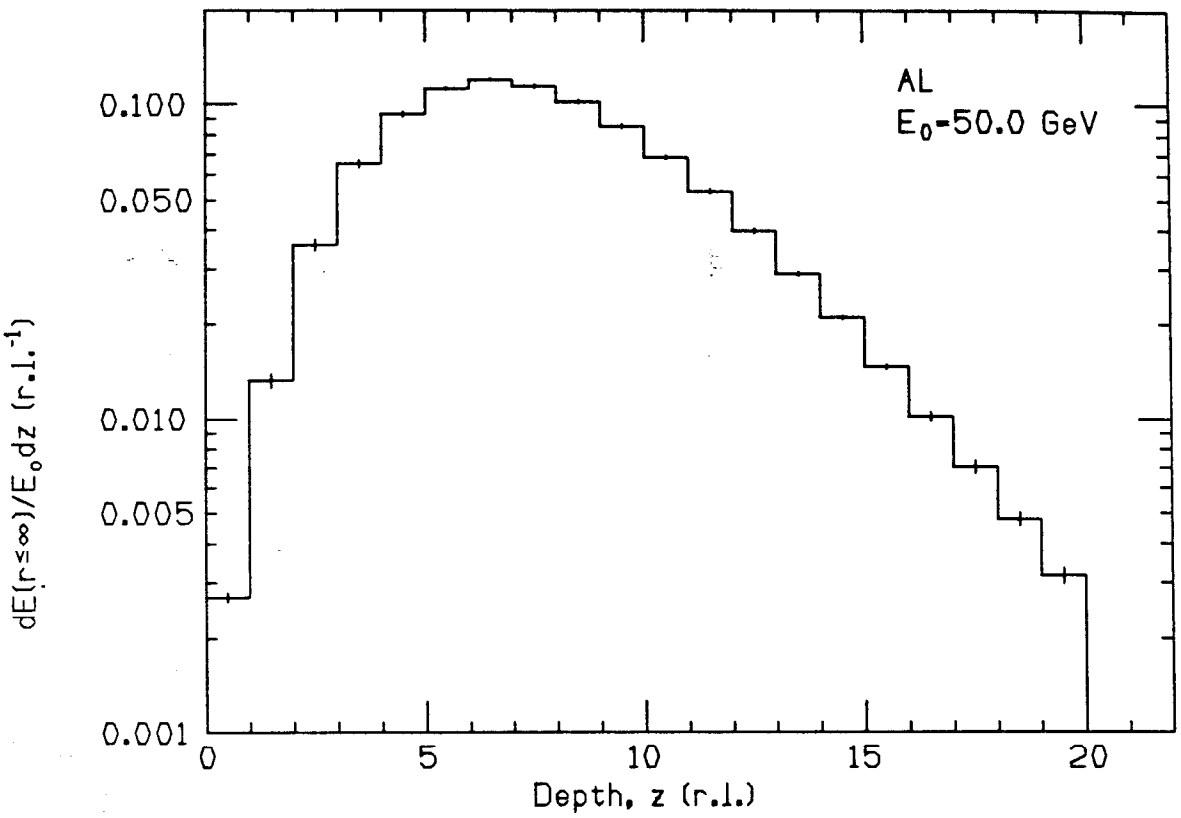

Fig. 15. Longitudinal E-deposition for aluminum.

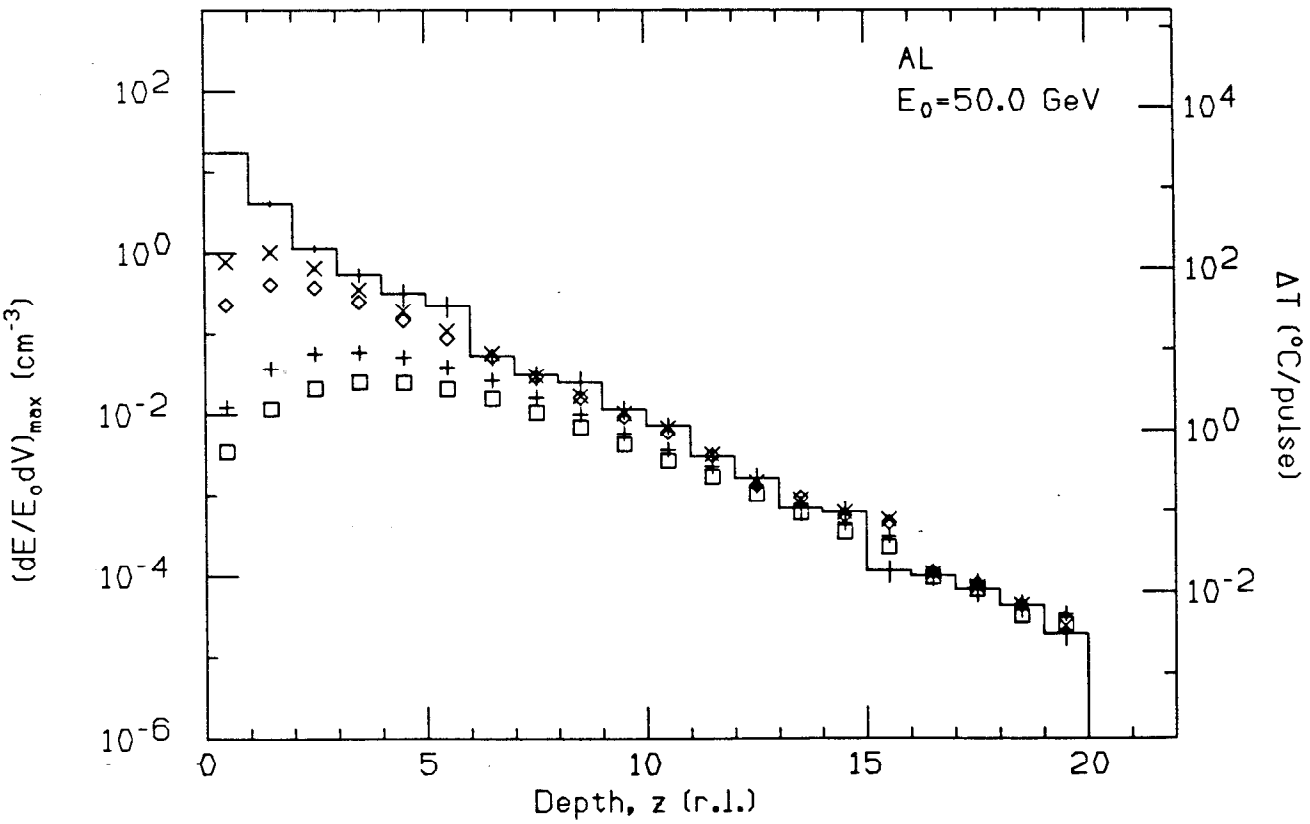

Fig. 16. Maximum E-deposition and temperature rise for electron beams of various sizes for aluminum.

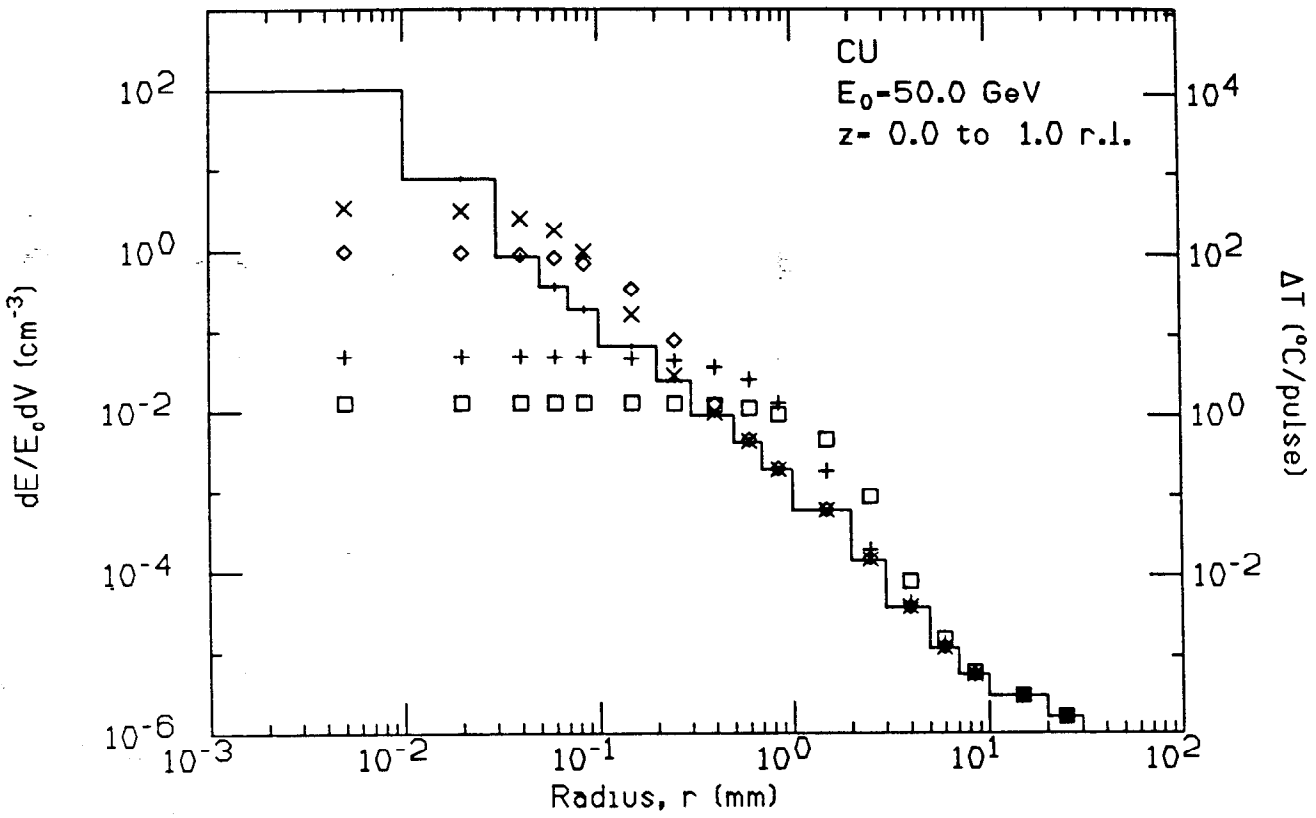

Fig. 17. E–deposition and temperature rise for electron beams of various sizes for copper at $0 < z < 1$ radiation lengths.

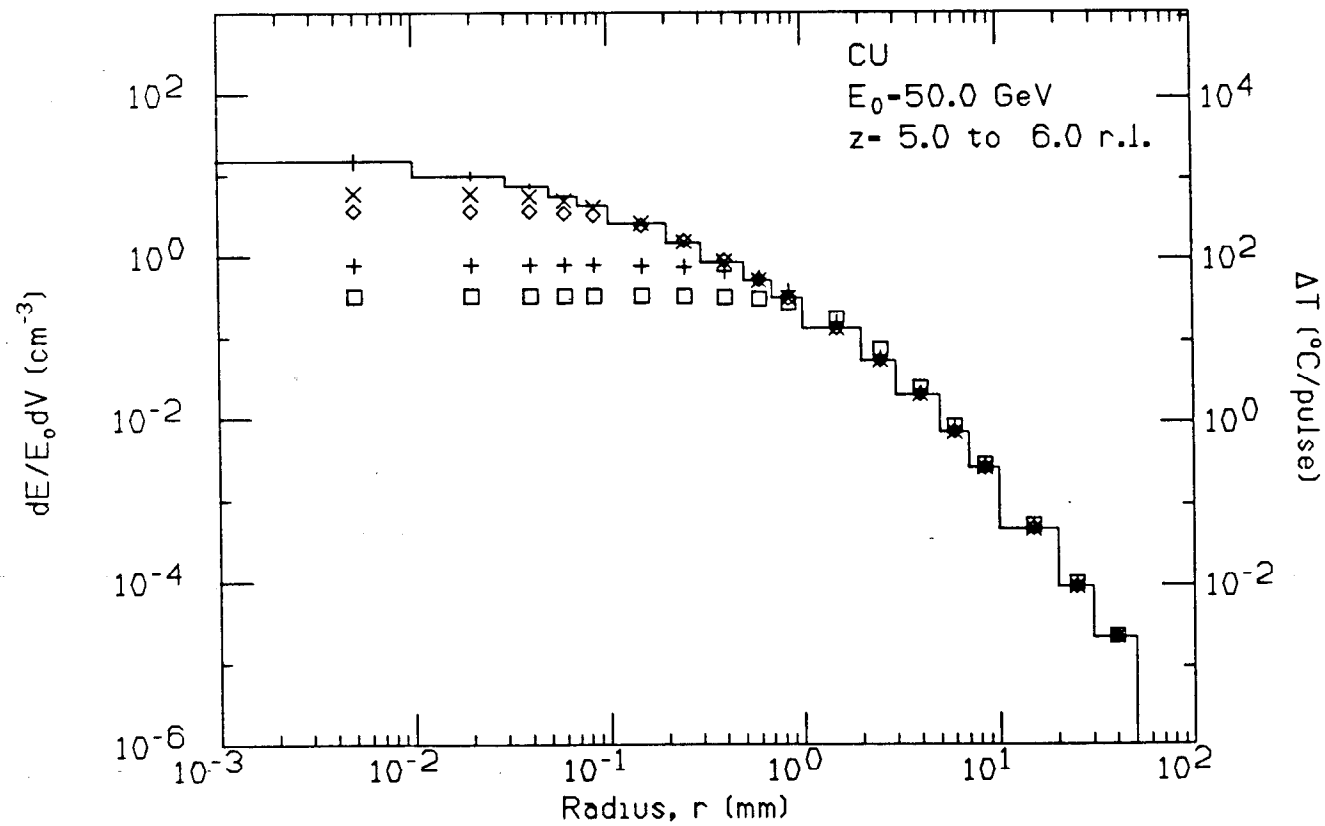

Fig. 18. E–deposition and temperature rise for electron beams of various sizes for copper at $5 < z < 6$ radiation lengths.

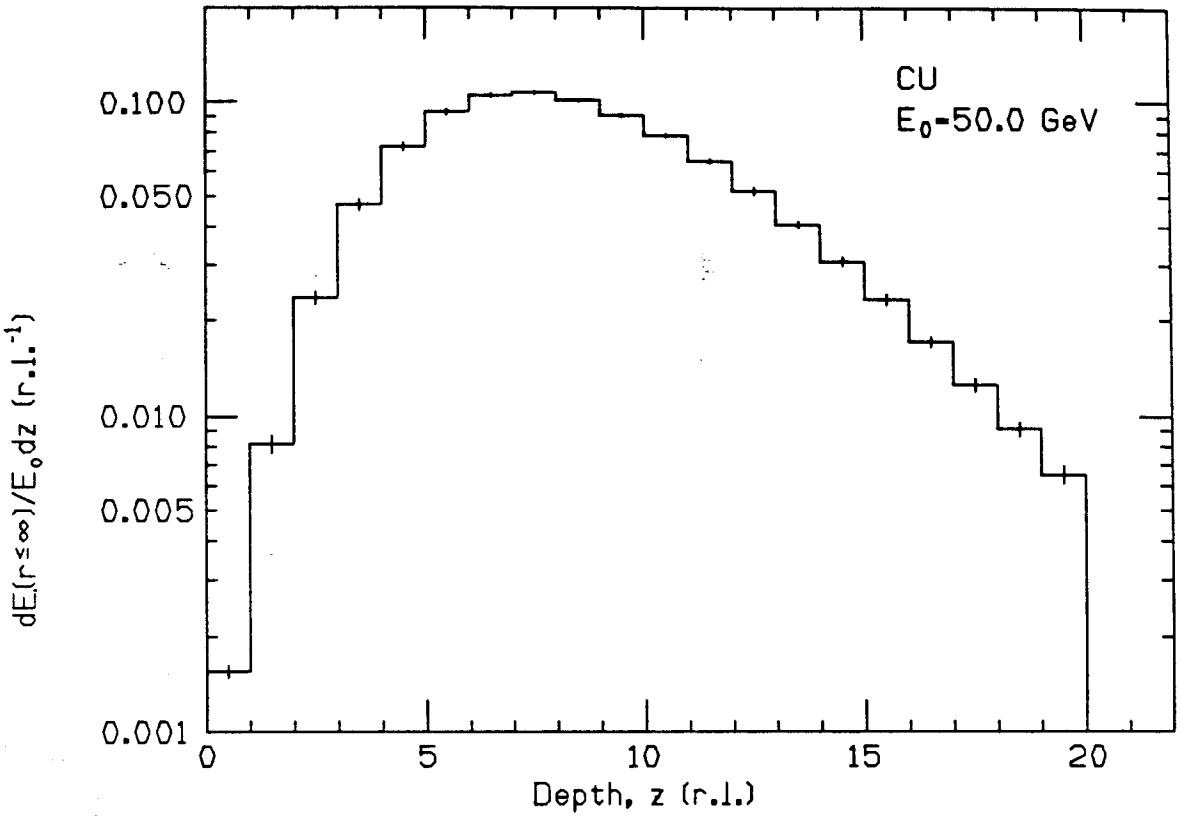

Fig. 19. Longitudinal E–deposition for copper.

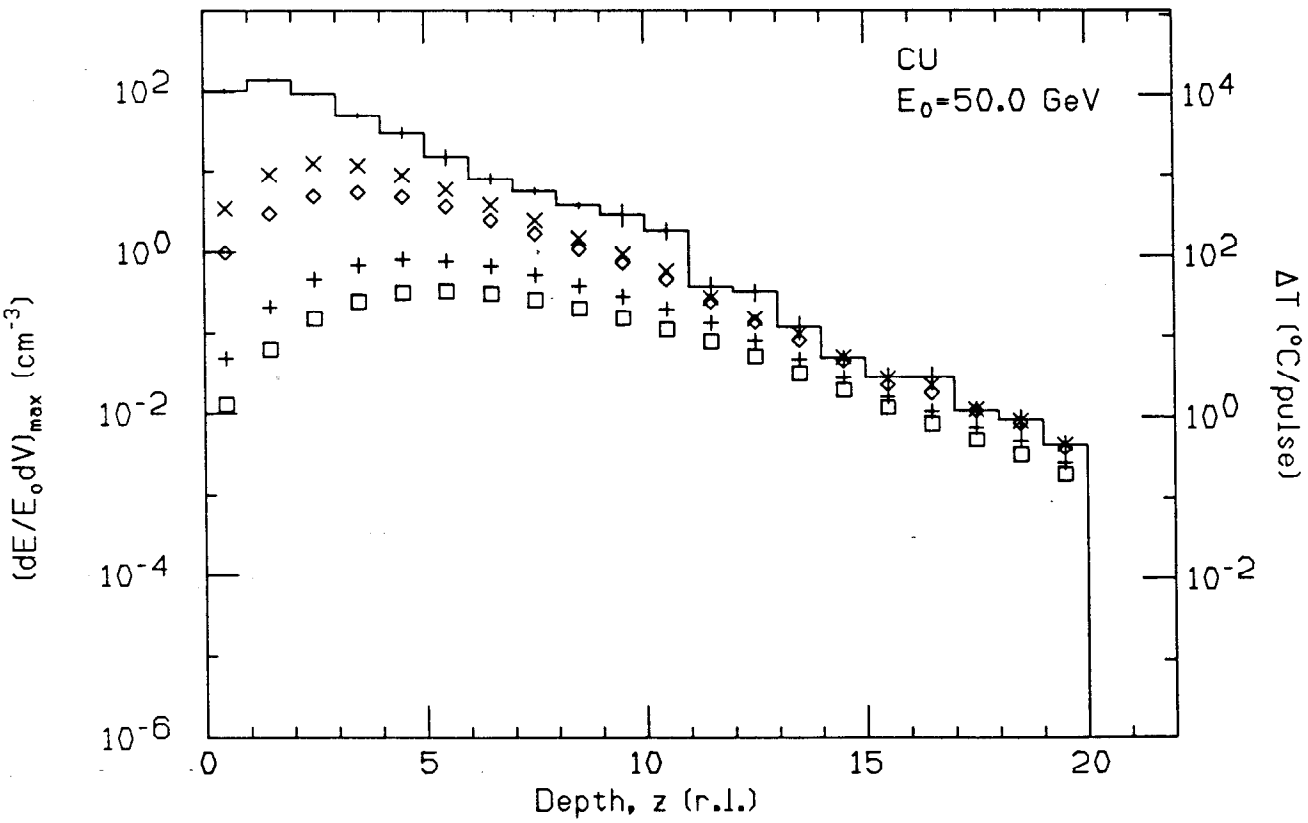

Fig. 20. Maximum E–deposition and temperature rise for electron beams of various sizes for copper.

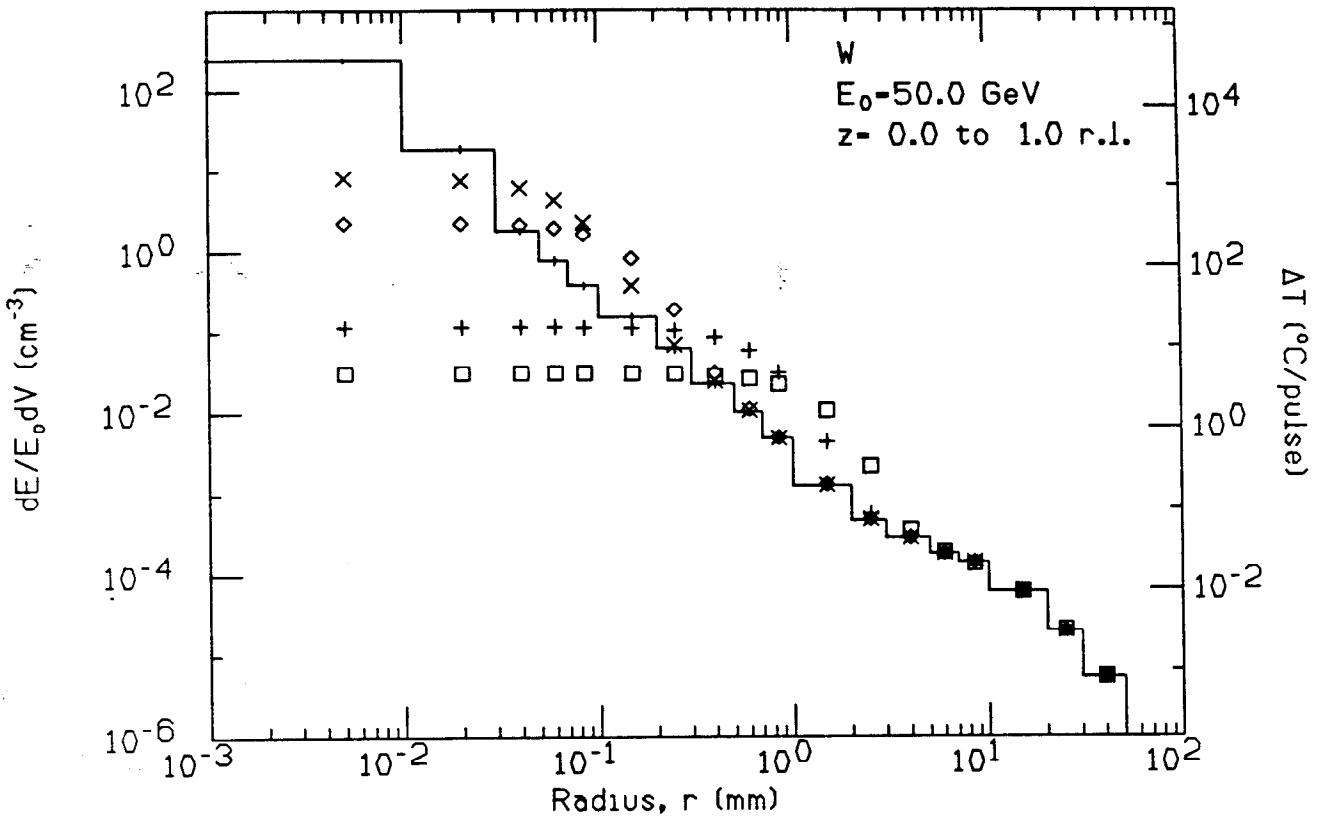

Fig. 21. E–deposition and temperature rise for electron beams of various sizes for tungsten at $0 < z < 1$ radiation lengths.

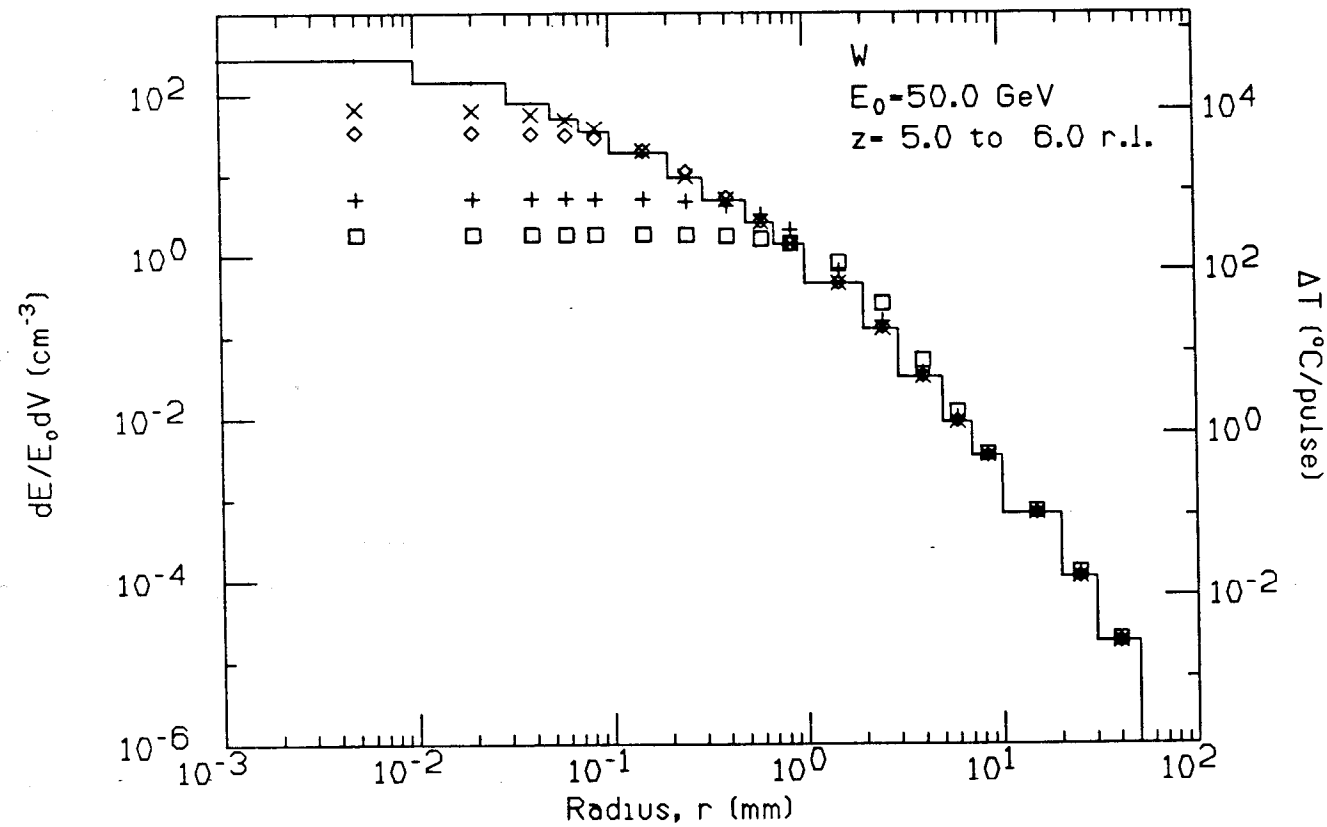

Fig. 22. E–deposition and temperature rise for electron beams of various sizes for tungsten at $5 < z < 6$ radiation lengths.

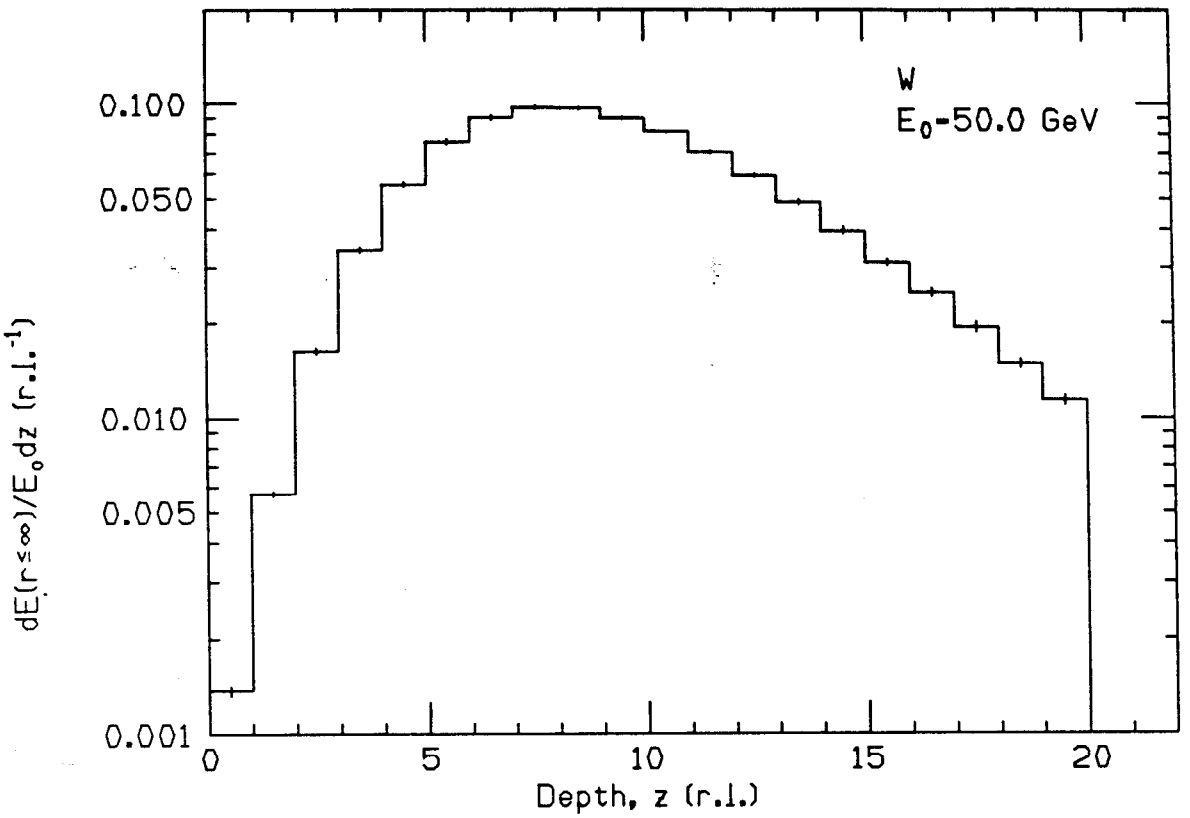

Fig. 23. Longitudinal E–deposition for tungsten.

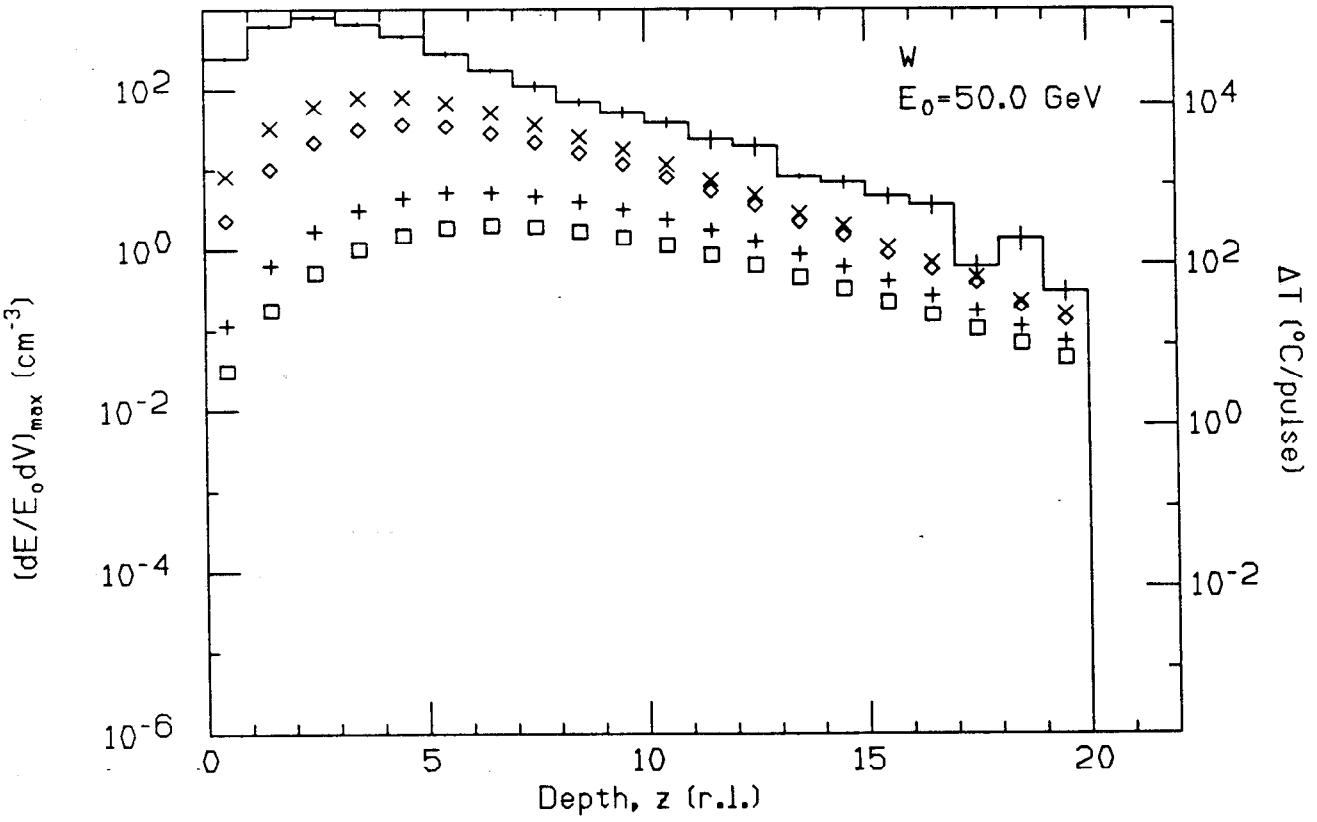

Fig. 24. Maximum E–deposition and temperature rise for electron beams of various sizes for tungsten.

Also important are the fatigue properties of the target material. Since most colliders have repetition rates of over 100 Hz, a target must withstand over 10^7 pulses per day of operation. This is essentially an infinite number of cycles when considering a fatigue curve (allowable stress versus cycles). In addition, some safety factor should be applied, *e.g.*, two or three times less stress than ultimate tensile strength, to account for imperfect materials, radiation damage, and other seen or unforeseen circumstances. Even with all precautions a target might structurally fail; hence its environment should be arranged to allow minimal damage to adjacent equipment and facilitate easy replacement or repair.

REFERENCES

1. Bruno Rossi, *High–Energy Particles,* Prentice–Hall, 1952.
2. W. R. Nelson, H. Hirayama and D. W. O. Rogers, *The EGS4 Code System,* SLAC–Report–265 (1985).
3. G. Brown, H. Winick, J. Harris and K. Halbach, Wiggler and Undulator Magnets, Nucl. Instrum. Methods **208**, 65–77 (1983).
4. U. Amaldi, *Proc. ICFA Workshop on Possibilities and Limitations of Accelerators and Detectors,* Les Diablerets, Switzerland, 1979; V. E. Balakin and A. A. Mikhailichenko, The Conversion System for Obtaining High Polarized Electrons and Positrons, Institute of Nuclear Physics, Novosibirsk, USSR Preprint 79–85 (1979).
5. J. C. Kimball and N. Cue, *Synchrotron Radiation and Channeling of Ultrarelativistic Particles,* Phys. Rev. Lett. **52**, 1747 (1984).
6. R. B. Neal, *The Stanford Two Mile Accelerator,* Benjamin, 1968; R. H. Helm and R. Miller, in *Particle Dynamics, Linear Accelerators,* p. 115–145, P. M. LaPostolle, A. L. Septier, Ed., North–Holland, Amsterdam, 1970.
7. Y. B. Kim and E. D. Platner, Rev. Sci. Instrum. **30**, 524 (1959); M. N. Wilson and K. D. Srivastana, *ibid.* **36**, 1096 (1965).
8. H. Lynch, SLAC, Private communication, 1984.
9. D. C. Carey, K. L. Brown and Ch. Iselin, *Decay Turtle,* SLAC–246 (1982).
10. W. B. Herrmannsfeldt and A. Drobot, private communication, 1984.
11. W. R. Nelson and S. Ecklund, *Energy Deposition and Thermal Heating in Materials Due to Low Emittance Beams,* SLAC–CN–135 (1981).
12. Stephan Timoshenko and J. N. Goddier, *Theory of Elasticity,* McGraw–Hill, 1951.